Applied Thermal Engineering 218 (2023) 119273

Contents lists available at ScienceDirect

Applied Thermal Engineering

journal homepage: www.elsevier.com/locate/apthermeng

Validation of a new methodological approach for the selection of wire-coil inserts in thermal equipment

A. García *, R. Herrero-Martin, J. Pérez-García, J.P. Solano

Departamento Ingeniería Térmica y de Fluidos, Universidad Politécnica de Cartagena, Campus Muralla del Mar, 30202 Cartagena, Spain

ARTICLE INFO

Keywords:
Methodology for wire-coil selection
Heat transfer enhancement
Wire-coil inserts
Transition Shape Parameter (TSP)
Friction factor
Enhanced flat-plate solar collector

ABSTRACT

The use of wire-coils is especially relevant at low Reynolds numbers (below the critical number to turbulent flow in smooth tubes) according to its inherent positive features such as the advance of transition onset and, if they present suitable geometric characteristics, the establishment of an extended transitional flow in a critical Reynolds number interval [Re_{CL} –Re_{CT}], with a predictable friction coefficient and Nusselt number. This paper presents the experimental validation of a new methodology based on the evaluation of a non-dimensional geometry-based parameter: the *TSP* (Transition Shape Parameter) that allows to predict the friction coefficient evolution with wire-coil inserts and enables to compute the extension of the transitional flow region. The close relationship between hydraulic and thermal performance of wire-coil inserts makes this methodology a valuable tool for selecting the most appropriate wire-coil geometry for a given tubular heat exchanger. It is observed that to promote an increase in heat transfer, the value of the Re_{CL} of the wire coil must be less than the operating Reynolds number range of the equipment. Thus, the Re_{CL} –Re_{CT} interval of the insert should fall into this range. In order to validate the methodological approach, an application to harp-type solar thermal collectors with typical Reynolds number range [40–6000] is presented. Four representative wire-coils, with a wide geometrical range characterized by TSP values of 759, 196, 35.3 and 3.1 (exhibiting significant differentiated behaviours in their friction factor curves and critical Reynolds numbers) were inserted inside the risers of a modified solar collector and experimentally tested at laboratory conditions. Static temperature at different locations at the absorber plate, and pressure drop were measured to obtain friction factor and Nusselt number inside riser covering the laminar, transitional and low-turbulent regions.

For a general application with friction factor constraints the most suitable wire-coil geometry is the TSP_{W02} = 196 with a range of critical Reynolds number of $Re_{CL} = 663$ and $Re_{CT} = 2286$ and $\overline{Nu}_{w02}/\overline{Nu}_s = 2.21$ for $Re = [300 - 3000]$ with $\overline{f}_{w02}/\overline{f}_s = 3,82$. However, for the case study presented (a harp-type solar collector) it is feasible to insert the third wire-coil geometry $TSP_{W03} = 35.3$ due to its early transition, with a range of critical Reynolds number of $Re_{CL} = 364$ and $Re_{CT} = 2324$, and $Nu_w/Nu_s = 1.35$ for $Re = 300$ with a high friction factor augmentation $\overline{f}_{w03}/\overline{f}_s = 18.84$. This geometry also promotes the highest absorber temperature reduction. The greatest temperature reduction is observed in the range of Reynolds numbers [700–2000], reaching approximately 6 °C, which represents approximately 15 %.

1. Introduction

The number of experimental studies regarding the thermo-hydraulic behaviour of wire-coil inserts using liquids as operating fluid is much lower than those that are focused on other tube-side enhancement techniques [15,20,2,4,27,11,26].

The wire-coils are a particular geometry that is classified differently according to their working regime. In laminar regime they are grouped as insert devices while in turbulent regime are classified within artificial roughness techniques (non-integral) along with other techniques such as corrugated and dimpled tubes (integral) [38].

In laminar flow, the dominant thermal resistance is not limited to a thin boundary layer adjacent to the flow. Thus, devices that mix the gross flow are more effective in laminar flow than in turbulent flow [38]. This has ruled out the wire-coils in front of other enhancement techniques that do mix the bulk flow such as twisted-tapes, mesh and brush inserts.

* Corresponding author.
E-mail address: alberto.garcia@upct.es (A. García).

https://doi.org/10.1016/j.applthermaleng.2022.119273
Received 13 May 2022; Received in revised form 26 July 2022; Accepted 2 September 2022
Available online 14 September 2022

Nomenclature

c_p	[J/kgK], Specific heat
d	[m], Inner tube diameter
d_h	[m], Hydraulic diameter
e	[m], Wire-coil thickness
f	–, Fanning friction factor
G	[kg/s], Mass flow rate
k	[W/mK], Thermal conductivity
l_e	[m], Hydrodynamic entry length
l_p	[m], Distance between pressure ports
p	[m], Wire-coil pitch
Δp	[Pa], Static pressure drop
T	[°C], Static temperature
t_m	[°C], Mean static fluid temperature in pressure tests
U	[m/s], Fluid velocity
$\acute{q}$	[W/m^2], Heat flux per square meter

Special Characters

β	[K^{-1}], Thermal expansion coefficient
ρ	[kg/m^3], Density
μ	[Pa.s], Dynamic viscosity

Parameters

Re	Reynolds number
Pr	Prandtl number
TSP	Transition Shape Parameter

Subscripts

CL	Critical laminar conditions (ending laminar flow regime)
CT	Critical turbulent conditions (beginning low turbulent flow regime)
H	High TSP
I	Intermediate TSP
in	Inlet conditions
L	Low TSP
m	Bulk flow conditions
out	Outlet conditions
s	Smooth
T	Turbulent fluid flow regime
Tr	Transitional fluid flow regime
p	Wall
w	Wire-coil

The wire-coils, like other artificial roughness techniques, advance the transition to turbulence, but have differentiating characteristics: usually, when the friction factor curves plotted against Reynolds numbers are observed, the integral roughness techniques present well-defined laminar and turbulent regions, and a sudden transition restricted within a narrow range of Reynolds number. Conversely, the wire-coil insert devices often present a more extended transitional region covering a wider range of Reynolds numbers. In this region, wire-coil inserts will typically have a much greater enhancement capability over integral roughness techniques. This fact represents a competitive advantage with respect to the aforementioned techniques. Despite, it has long been considered that the wire-coils are not a suitable technique to enhance heat transfer within smooth tube under laminar regime, if the appropriate wire-coil geometry is chosen, a transition regime at low Reynolds numbers can be achieved with a moderate friction factor increase, in many cases lower than that obtained from other inserted devices that produce greater flow obstruction.

In fully turbulent flow, the wire-coils enhancement mechanism (separation and flow reattachment) is analogous to that of the integral roughness techniques but typically, they present a larger shape resistance, which entails greater friction factor increases with respect to dimpled and corrugated tubes, so these are commonly used. In this region, integral roughness techniques have been much more studied. In fact, many of the studies employing wire-coils under turbulent regime were devoted to simulate integral roughness. However, in many occasions, at intermediate Reynolds numbers, the hydraulic behaviour of the wire-coil inserts differs substantially from that presented by the integral roughness techniques, as the shape of the roughness strongly influences the pressure drop characteristics. Normally, the wire coil-inserts advance the transition to turbulence in comparison with integral roughness techniques, due to its inherent geometrical roughness shape [9].

The number of studies of wire-coil inserts under laminar regime is very limited. Accordingly, the available correlations to predict friction factor in laminar flow are scarce. Besides, in some cases, the validity ranges, in terms of Reynolds numbers, are not specified, and in others, the correlations are only valid for the singular geometries under study. Importantly, some of them are obtained from the analysis of a limited number of wire-coils. Chen and Zhang [3]; Nazmeev et al [19] and García et al. [6–7] positively contributed to this field. More recently, Akhavan-Behabadi [1] and Roy and Saha [24] proposed their own friction factor correlations. The correlation proposed by Akhavan-Behabadi was established for 2 mm thickness wire coils and was just a function of Reynolds numbers from [20–39]. Roy and Saha presented a generalized correlation as a function of the helix wire-coil angle and the dimensionless thickness for Re [15–39] but they only tested three wire-coils.

The number of correlations for friction factor in turbulent flow available in the open literature is higher that the corresponding to laminar flow as those proposed by Sethumadhavan and Rao [29], Zhang et al [39], Inaba et al. [13] and García et al. [6]. Furthermore, the turbulent ones are more reliable. More recently, Jafari Nasr et al. [14], San et al[28],Sharafeldeen et al. [30]published new correlations. Nevertheless, in the optimum wire-coil operating range (transitional and low turbulent regime Re $\leq$ 4000), the information is scarce.

From the year 2000, the most well-known works on single phase heat transfer enhancement by employing wire coils are those of Wang and Sunden [37], García et al [6–9], Naphon [18], Promvonge et al [22] and Gunes et al [10]. In a recent review on heat transfer and flow mechanisms within enhanced heat exchangers, Kumar et al [17] mentioned that wire coils are beginning to gain popularity due to their low cost and good performance. Nevertheless, the works that have appeared recently are developed under smooth tube turbulent flow, such as those by San et al [28] or Hong et al [12]. San et al [28] presented heat transfer and pressure data employing air and water as working fluids. They tested nine wire-coils and proposed two heat transfer empirical equations for air valid for Re (3718–17157); p/d (1.304–2.319); e/d (0.0725–0.134) and for water valid for Re (5510–15080); p/d (1.304–2.319); e/d (0.0725–0.134). Hong et al [12] performed thermal and pressure drop tests for 13 different wire-coil inserts employing air as the working fluid for Reynolds numbers ranging from 6000 to 20,000.

As previously exposed, the thermal correlations available have basically been obtained for turbulent flow, where the wire-coils show their worst enhancement potential. The development of correlations for smaller Reynolds numbers is much more complicated by the presence of different flow regimes [7] and of different thermal mechanisms (mixed and forced convection). This lack of availability prevents a more widespread use [7]. In this context, Pérez-García et al [21] used a large experimental database of the friction factor for a wide wire-coil geometric range with data covering all flow regions (laminar, transitional

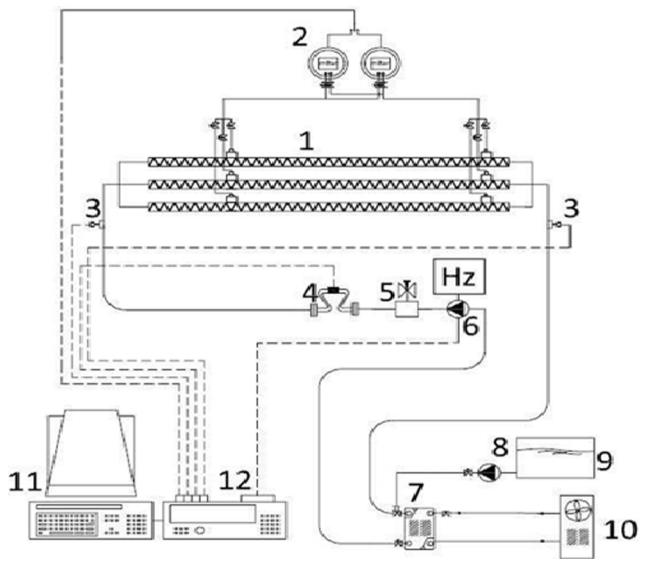

Fig. 1. Test section layout for friction factor (1) Tubes with inserted devices test section (2) Differential manometers (low and high pressure ranges) (3) Temperature sensors (4) Coriolis Mass Flowmeters (5) Regulator Valve (6) Centrifugal Pump (7) Flat Plate Heat exchanger (8) Filling pump and (9) Water tank (10) Chiller.

and low turbulent), and established new correlations to predict the critical Reynolds numbers that delimit the ending of the laminar region (Re_{CL}) and the beginning of the turbulent region (Re_{CT}) as functions of the inserts' geometrical parameters. Likewise, the authors grouped the wire-coil inserts by families based on the evolution of the observed friction factor and proposed a new geometrical based dimensionless number, the Transitional Shape Parameter (TSP), that allows to infer the wire coils' hydraulic behaviour. Additionally, specific friction factor correlations according to the insert TSP value were developed for the different flow regions.

More recently, different approaches have been reported in the literature. Provonge et al (2022) studied the thermal–hydraulic performance of a solar receiver heat exchanger equipped with a new design of longitudinal-vortex generator placed on the absorber, using air for Re (5000–25000). Wang et al [36] explore experimentally the effect of turbulent pulsatile flow in a serpentine channel with an innovative winglike turbulators for Re = 10000 and finally, Verma et al [34] carried out a numerical study to predict the transient thermal performance of a PCM embedded parallel flow solar air heater during a 24 h working cycle. Artificial intelligence methods have been employed to predict the thermal and hydraulic characteristics in enhanced heat exchangers [32]. For twisted-tapes the use of response surface method (RSM), genetic algorithm, and Taguchi approach has also been applied [16]. To find the most adequate wire-coil insert to enhance a heat exchanger, Sharifi et al [31] employed 3D numerical simulations, artificial neural network (ANN) and genetic algorithms (GA) and Subasi and Erdem [33] introduced as an integrated optimization methodology, a hybrid approach that combines Multi-objective Optimization and Multiple-criteria Decision-making techniques.

In summary, as stated by Sharifi et al [31], many works have studied wire-coil inserts and concluded that they were a feasible enhancement technique for heat-exchangers, but they have not provided a clear approach to find and select the optimum helical wire at specific conditions to enhance the overall efficiency of heat-exchangers.

This paper presents the experimental validation of the proposed methodological approach for wire-coil selection. It is based on the direct relationship between the hydraulic and thermal behaviour of wire-coils being used as a passive heat transfer enhancement technique. The experimental tests carried out for validation purpose were performed using a modified harp type flat-plate solar collector. This case study is a very interesting engineering application, since the fluid flow regime can be laminar, transitional or low turbulent, depending on the operating conditions. The experimental tests performed were aimed to obtain; the static temperature at different locations at the absorber plate, and the pressure drop and the heat transfer rate inside the modified risers of a solar collector equipped with four different geometries of wire-coil inserts characterized by the following TSP values: 759, 196, 35.3 and 3.1, in order to have a full representation of the different categories.

2. Experimental set-up

The experimental set-up to carry out friction factor and heat transfer tests is described in Figs. 1 and 2.

Two closed circuits are connected through a flat-plate heat exchanger (7). The main circuit for friction factor tests contains the test section in which the smooth tubes and the tubes with inserted devices are tested (1). In this main circuit; pressure (2), temperature (3) and mass flow rate (4) data are monitored. The flow is pumped (6) to the test

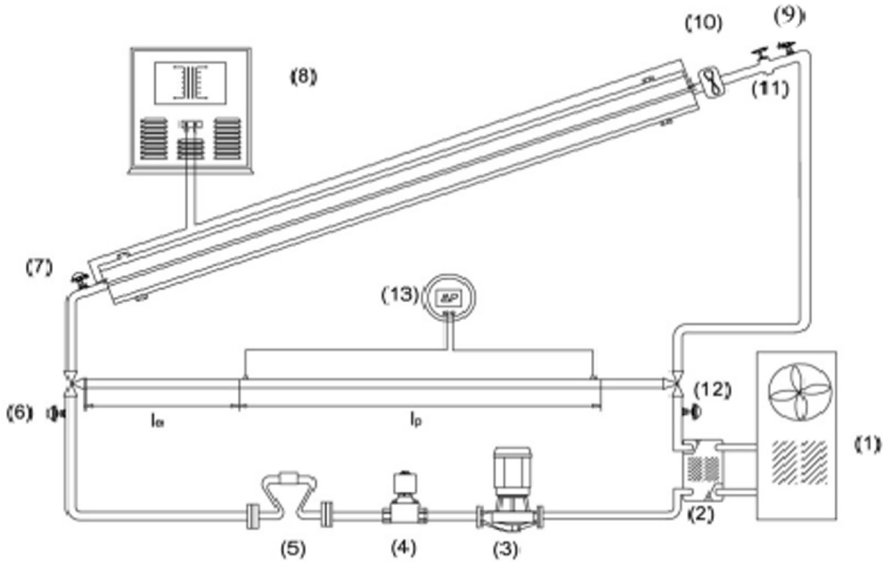

Fig. 2. Test section layout for heat transfer.

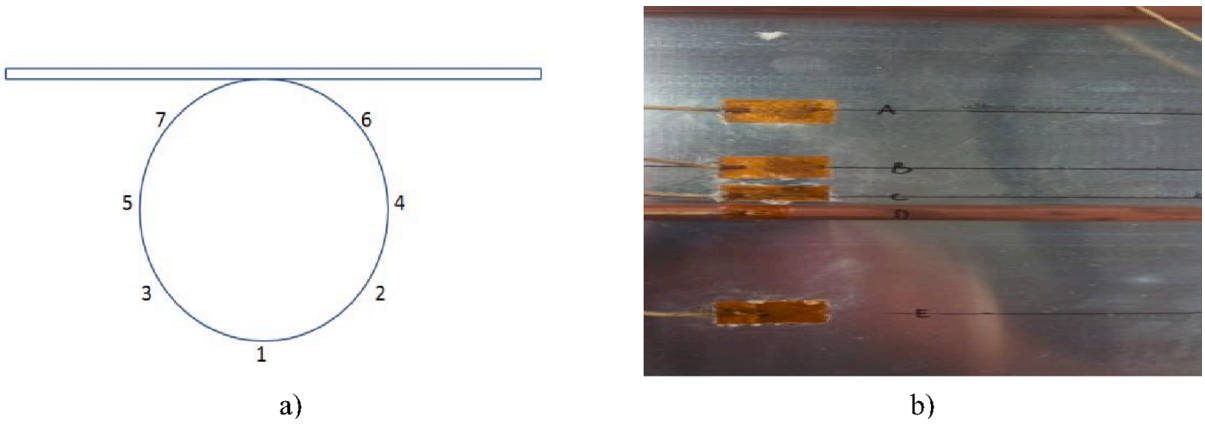

Fig. 3. Test section details: (a) Heat transfer test section J, location of the thermocouples, (b) Heat transfer absorber test section. Axial location at 1290 mm.

Table 1
Classification of the wire-coils according to the dimensionless parameter TSP:

Wire-coil	d (mm)	p (mm)	e (mm)	p/d	e/d	p/e	TSP	Classification
W01	7	10.5	0.7	1.50	0.100	15.00	759.0	TSP > 750
W02	7	7.0	0.5	1.00	0.007	14.00	196.0	10 < TSP < 750
W03	7	7.5	1.4	1.07	0.200	5.36	35.3	10 < TSP < 750
W04	7	3.5	0.7	0.50	0.100	5.00	3.1	TSP < 10

section where three tubes with wire-coil insert devices are tested. Each tube has two pressure taps separated from each other 1.4 m, in order to compute the average pressure drop at the differential pressure manometers. These manometers allow different pressure range measurements. The LD301 Smar (lower pressure range) allows to carry out laminar flow measurements in inserted tubes up to 50 mbar and the LD303 Smar (higher pressure range) for turbulent flow measurements up to 500 mbar. In Annex II, the uncertainty analysis procedures and the measurement accuracy including the technical data by the manufacturers are provided.

Due to the need to perform tests at different temperatures, it is essential to include a secondary circuit in the test-bench that keeps the main circuit flow at the established test temperature. In order to carry out heat transfer tests, the angle of inclination of the three tubes test-section with inserted wire coils is modified to be representative of the real operating conditions in solar collectors. The section is upper heated by means of an electrical blanket.

Two heat transfer sections are measured. The total length of the riser is 1900 mm. Section J (See Fig. 3a) is located 1610 mm downstream of port inlet, and seven thermocouples are located peripherally at the outer tube wall. The second test section is located at the absorber panel (See Fig. 3b) at 1290 mm from the inlet. In this cross section, 4 thermocouples are placed on both sides of the central tube and one on the central tube. The first sensor, thermocouple A, is located 55 mm to the left of the central tube. The thermocouple E is placed symmetrically to the A on the right side. The thermocouples B and C are placed on the left side at 25 and 10 mm from the tube, respectively. Finally, thermocouple D is placed at the tube wall.

3. Methodology

The methodology proposed is aimed to provide a criterion to select, from a set of possible wire-coil geometries, defined by their dimensionless pitch (p/d), and thickness (e/d), the most feasible ones according to the operating conditions of the thermal equipment. When selecting a wire-coil for a given problem, the operating flow rate of the equipment as well as the permissible increase in the friction factor must be taken into account.

As a result, the optimal wire coil for a given application will be the one that, due to its geometric characteristics, develops an extended transition region as wide as possible, and that fits within the range of Reynolds numbers of the application under study, also maintaining a friction coefficient as low as possible that remains almost constant.

All the wire-coils presents a purely laminar region up to Re_{CL} (beginning of the transition region). In this region, it is expected that the wire-coils show a non-remarkable thermal enhancement and would not be the optimal working region, because of a limited flow disturbance. Within the transition region, it can be steadily developed over a wide region of Reynolds numbers or, in some cases, it can present a sharp transition (as that typically displayed by smooth tubes) but the onset of transition occurs at much lower Reynolds numbers. In some cases, in this transition region, a gradual increase in the friction factor with the Reynolds number can be observed, while in other cases the friction factor remains practically constant between the interval Re_{CL}-Re_{CT} [21]. In summary, for a given heat transfer equipment, the best thermal performance is expected for the wire coil inserts which exhibit this last characteristic behaviour of the friction factor within the equipment working Reynolds range.

The application chosen for validation purposes was a solar thermal collector, as it presents a wide variability of flow regimes, and the associated heat transfer mechanisms are complex [5]. This is due to its inherent variable characteristics, such as: the working mode (forced circulation or thermosyphons), the flow regime (laminar, in transition or turbulent), the collector type (harp or serpentine), the working fluid properties (from 100 % water to 50 % mix water-glycol) and the operating temperature (15 to 90 °C). For a specific application, the typical operating ranges of the flat-plate solar collector should be well known to accurately select the optimal wire-coil insert.

In this work, a flat plate solar collector which uses water as the heat transfer fluid in a temperature range between 15 and 40 °C, and a mass flow rate per tube between 0.3 and 50 kg/h has been studied. The corresponding Reynolds number range is Re = 40–6000. The heat flux applied at the absorber plate is 800 W/m^2. A set of four wire-coil geometries have been considered for heat transfer enhancement in this thermal equipment (See Table 1).

The validation of the methodology proposed for selecting the geometrical characteristics of the optimal wire-coil for a specific application is summarized in Fig. 4 and consists of the following steps:

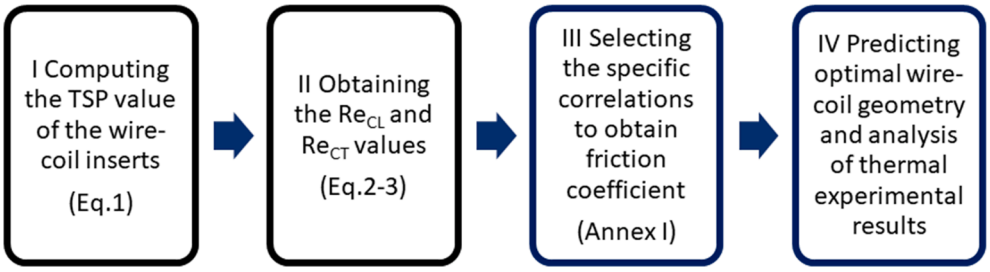

Fig. 4. Graphical representation of the proposed methodology.

Table 2
Critical Reynolds numbers for laminar and turbulent flow (predicted and experimental values).

		Re_{CL}			Re_{CT}		
Wire Coil	TSP	Correlations	Experimental	Rel. Error (%)	Correlations	Experimental	Rel. Error (%)
W01	759.0	509	500	1.8	2516	2300	8.6
W02	196.0	663	675	1.8	2286	2150	5.9
W03	35.3	364	355	2.5	2324	2300	1.0
W04	3.1	638	630	1.3	1936	1890	2.4

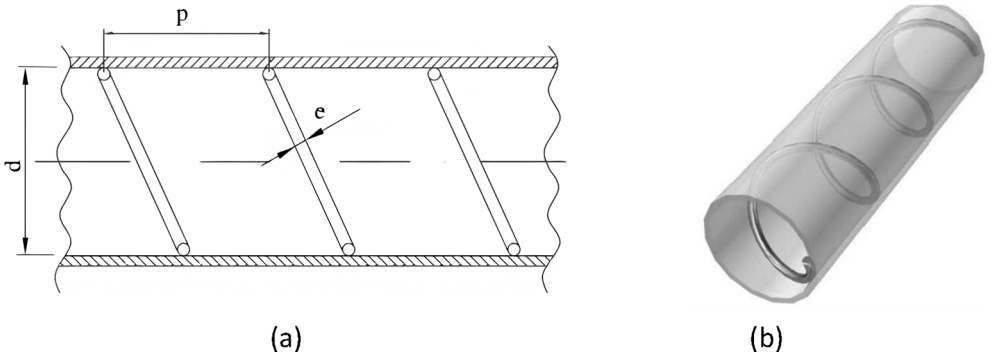

Fig. 5. (a) Wire Coil Geometry. (b) Sketch of a wire coil inserted inside a smooth tube.

I. Computing the TSP (Eq. (1)) value of the wire-coil inserts candidates according to the range of Reynolds number for a specific application
II. Obtaining the critical Reynolds numbers of the ending of laminar flow region (Re_{CL}) and begining of the turbulent flow region (Re_{CT}) (Eq. (2), (3)) and comparing with experimental results
III. Selecting the specific correlations to obtain friction coefficient (Annex I) and comparing with experimental results plotting friction curves in the different flow regions
IV. Predicting optimal wire-coil geometry and analysis of thermal experimental results

As aforementioned, the range of operating Reynolds numbers in the application under study should overlap as closely as possible with the range of the extended transition region generated by the wire-coils. This can be predicted by using the correlations of the critical Reynolds numbers and those which provides the evolution of the friction coefficient, which are dependent of the TSP parameter and therefore on the geometric characteristics of the insert. In this case, for the validation of the methodology, what has been done was to select four wire coil inserts, representative of each one of the different TSP categories (High, Intermediate, Low). The geometric characteristics of these four wire-coils are summarized in "Table 1" and later in "Table 2" the limit values of the extended transition region are computed. The TSP definition and correlations employed in this section (Eqs. (1)–(3)) were obtained from Pérez-García et al work [21].

I. Computing the TSP value of the wire-coil inserts

Fig. 5 depicts the wire coil geometrical parameters and a Sketch of a wire coil inserted in a smooth tube.

The dimensionless parameter TSP (Transition Shape Parameter) enables the classification of the wire-coil inserts. It is defined as:

$$TSP = \frac{(p/d)^5}{(e/d)^2} \tag{1}$$

In Table 1, the dimensionless parameter TSP is presented for each wire-coil employed allowing to classify them according to the computed values.

The TSP allows to predict the different evolution of the friction factor coefficient with Reynolds number in the transition region, in comparison with smooth tubes. From Pérez-García et al [21] work, the following friction factor trends are expected for the specimens tested:

- W01: a wire-coil insert with a TSP > 750 (High), a non-abrupt change in tendency is expected within transition and extends over a wide region of Reynolds numbers.
- W02 and W03: grouped in 10 < TSP < 750 (Intermediate), the evolution of friction factor presents different trends, but the dominant factor is the dimensionless thickness. Thus, for e/d < 0.1 the friction factor is expected to smoothly rise in the transition region, whereas for e/d = 0.2 it remains constant in the transition region.

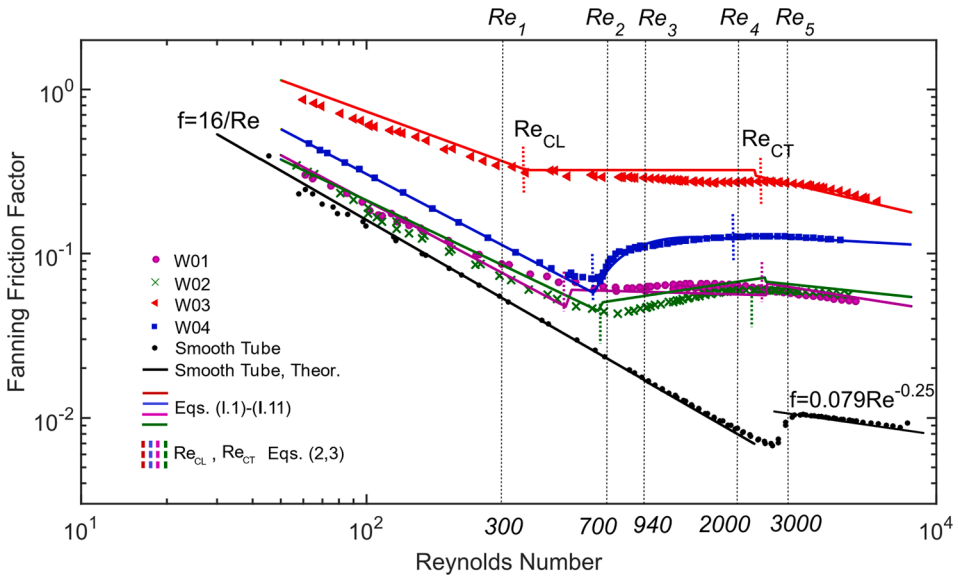

Fig. 6. Friction factor evolution. Experimental results, Re_{CL}, Re_{CT} and correlations.

Table 3
Average percentage errors for wire coils, smooth tube (correlation data vs empirical data).

	Laminar region				Trasitional region				Turbulent region			
	Max. error Correl.	Max Dev.	Average Error correl.	Dev. Aver.	Max. error Correl.	Max Dev.	Average Error correl.	Dev. Aver.	Max. error Correl.	Max Dev.	Average Error correl.	Dev. Aver.
W01	9.3 %	10.0 %	6.5 %	3.2 %	22.9 %	13.8 %	9.2 %	8.9 %	23.6 %	10.0 %	8.4 %	7.5 %
W02	12.1 %	18.2 %	7.7 %	10.7 %	14.1 %	17.3 %	6.7 %	12.5 %	14.9 %	10.3 %	7.7 %	8.5 %
W03	18.0 %	7.8 %	1.5 %	2.1 %	14.1 %	16.1 %	6.7 %	12.4 %	4.0 %	6.2 %	0.3 %	2.0 %
W04	6.4 %	20.7 %	3.9 %	4.5 %	23.4 %	12.7 %	16.5 %	2.1 %	6.9 %	3.1 %	3.1 %	0.4 %
Smooth		7.0 %		1.0 %						3.5 %		2.5 %

- W04: a wire-coil insert with a TSP < 10 (Low) as an enhancement device, the friction factor reflects the smooth tube behaviour. Thus, an abrupt rise of the friction factor in the transition region is predicted.

II. Obtaining the critical Reynolds numbers of the ending of laminar flow region (ReCL) and begining of the turbulent flow region (ReCT)

The correlations to predict the critical Reynolds numbers for ending laminar flow regime (Eq. (2)) and beginning of low turbulent flow regime (Eq. (3)) are:

$$Re_{CL} = 5.710(p/d)^{-2.407} + 144.229(p/d)^{-0.167}(e/d)^{-0.575} \quad (2)$$

$$Re_{CT} = -347.213 + 2633.779(p/d)^{0.206} \quad (3)$$

The results obtained are shown on Table 2 and also the experimental values are provided for comparison purposes. They allow to assess the following hydraulic behaviour for the specimens tested:

III. Selecting the specific correlations to obtain friction coefficient

The employed correlations allow to accurately predict the friction factor curve evolution in the different flow regimes without the need of carrying out experimental tests as depicted in Fig. 6. For validation purposes the friction factor curve for each insert has been experimentally obtained for Re = 60–6000. The analysis will focus on five representative Reynolds numbers: 300, 700, 940, 2000, 3000.

Table 3 shows the average deviation for the wire-coil insert devices studied of the correlated against the experimental data. The experimental procedure has been validated through smooth tube testing. There is a good agreement between the analytical and the experimental results of the smooth tube, thus ensuring the validity of the measurement procedure. The maximum error encountered at Re = 60 represents a 7 % deviation regarding the theoretical laminar solution.

IV. Predicting optimal wire-coil geometry and analysis of thermal experimental results

The information obtained through a detailed analysis of the friction factor curves allows to select the most appropriate insert geometry for a given application. In Fig. 6 it is highlighted the end of the laminar region (characterized by $Re_{CL,}$) and the beginning of the fully turbulent regime (characterized by Re_{CT}) for each wire coil studied. Between Re_{CL} and Re_{CT} the friction factor curve shows an almost constant slope. The W03 specimen is the one that most disturbs the flow due to its high e/d ratio, markedly anticipating the end of the laminar regime (Re_{CL} = 364) showing the widest range between Re_{CL} and Re_{CT} followed by W01, W02 and finally W04.

The wire-coils with intermediate and high TSP values present smoother transitions with a wider Reynolds numbers range where the friction curve does not show a change of trend (extended transition region). This suggests a predictable hydraulic behaviour of these devices in that region. Solar collectors typically experiment wide temperature fluctuations which entails large Reynolds number variation. The aforementioned wire coils would be a good option assuring that their Re_{CL} - Re_{CT} interval matches the operating solar collector Reynolds number range. It is shown how wire coil with the lowest TSP (W04) presents an abrupt transition to turbulent flow. This specimen will have an uncertain behaviour around its critical laminar Reynolds number, which clearly makes inadvisable its use within solar collectors working at those mass

Table 4
Friction factor increase (f_w/f_s) for the wire-coils studied.

fw/ fs	(Re = 300)	(Re = 700)	(Re = 940)	(Re = 2000)	(Re = 3000)	Average
W01	2.0	2.6	3.5	8.0	5.4	4.30
W02	1.3	1.9	2.8	7.5	5.6	3.82
W03	5.9	12.3	17.0	34.0	25.0	18.84
W04	2.0	3.6	6.5	15.6	12.0	7.94

flow rate ranges.

Due to the direct link between the flow pattern and the heat transfer, the calculation of the TSP, Re_{CL} and Re_{CT} and friction factor evolution allows to infer the expected thermal behaviour of an equipment with wire coil inserts in relation to the standard one.

In the laminar region ($Re < Re_{CL}$) the wire-coils do not disturb the flow enough to promote a significant rise in heat transfer. As soon as a given wire coil promotes transition ($Re > Re_{CL}$) heat transfer will be increased. In a smooth tube working at a given Reynolds number, the highest heat transfer augmentation will be obtained if there is laminar

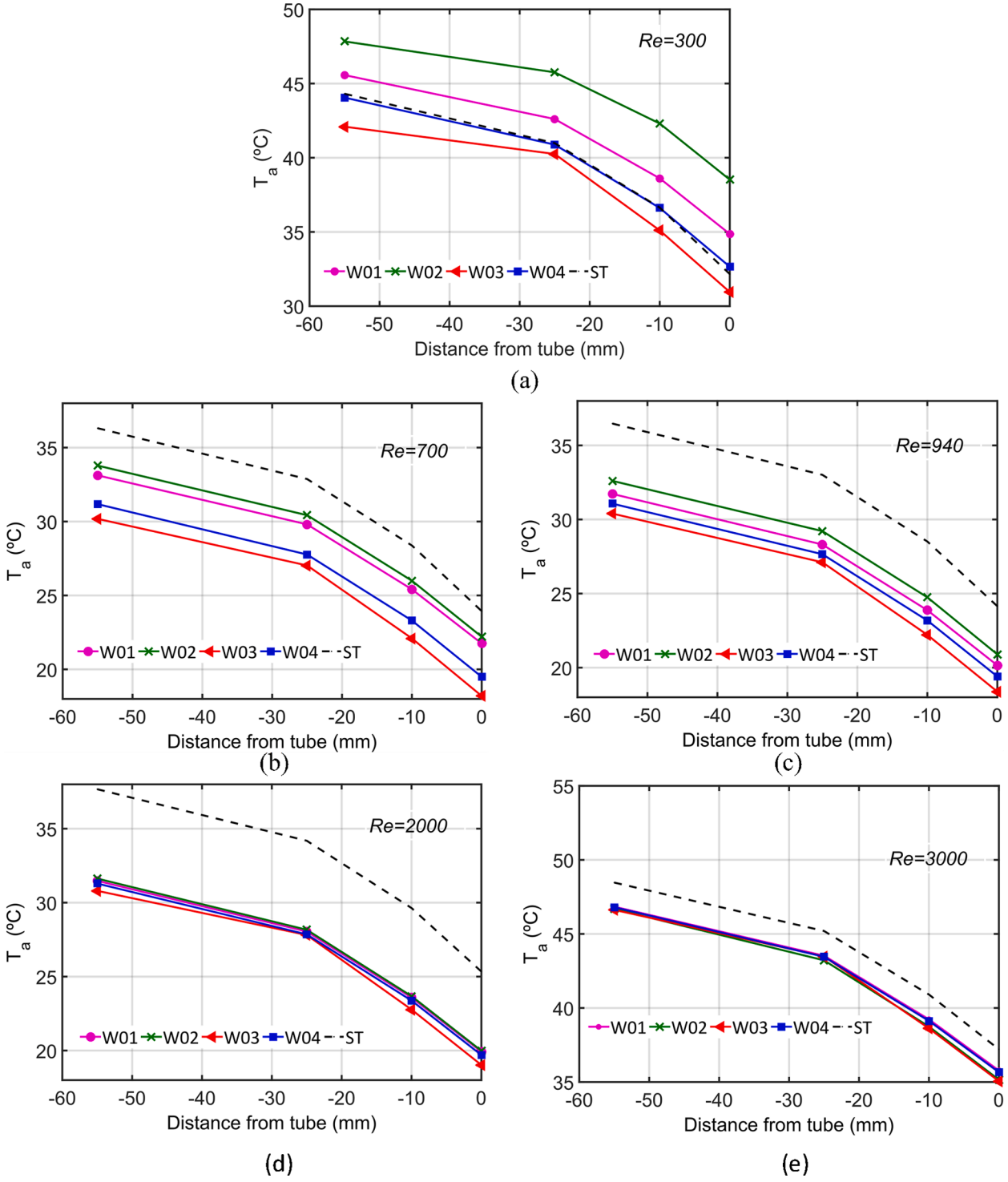

Fig. 7. Thermal results at the absorber plate for Re = 300–3000.

Table 5
Nusselt number values at section J and associated uncertainty value for Re = 250–3000.

	Re = 300		Re = 700		Re = 940		Re = 2000		Re = 3000		Average
	Nu	u_{NU}(%)	Nu	u_{NU}(%)	Nu	u_{NU}(%)	Nu	u_{NU}(%)	Nu	u_{NU}(%)	Nu_w/Nu_s
Smooth	6.5	0.43	7.0	0.54	6.9	0.58	6.5	0.9	14	3	
W01	4.6	0.25	10.8	1.20	20.8	5.03	51.3	50.9	–	–	2.67
W02	2.9	0.18	9.8	0.83	16.3	2.40	48.9	42.9	–	–	2.38
W03	8.8	0.83	–	–	–	–	–	–	–	–	1.08
W04	5.0	0.31	24.2	6.56	34.0	16.74	–	–	–	–	2.58

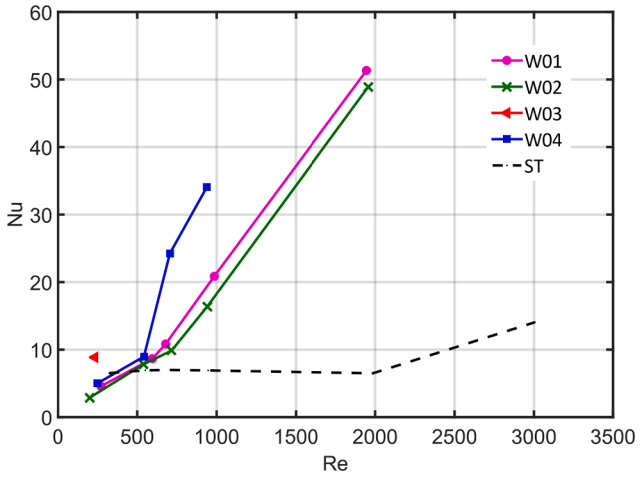

Fig. 8. Nusselt number values vs Reynolds number at section J.

flow at the smooth tube and either transitional or turbulent flow when a wire coil is inserted. When the smooth tube is at turbulent regime, the use of wire coils will have a reduced impact on heat transfer augmentation that in many cases do not compensate the increase in pressure drop.

The increase in pressure loss produced by the inserts is an important factor to be considered depending on the application where the heat exchanger is installed. In order to focus the study, five representative Reynolds numbers were studied: 300, 700, 940, 2000, 3000, as highlighted in Fig. 6.

Table 4 displays the results obtained in terms of friction factor increase in comparison with smooth tube results f_w/f_s. The wire coil W03 is the one that induces significantly higher pressure drop, accounting for 6 to 34 times the head losses of the smooth tube, due to its high e/d value. The wire-coils W01 and W02 produce more moderate increases, up to 8 times the pressure loss of the smooth tube. As expected, the maximum increases are observed when there is turbulent regime with wire-coils and still laminar flow in the smooth tube (Re = 2000).

For Reynolds numbers around 300, the only insert capable of significantly disturbing the flow is W03 with a Re_{CL} of 364. However, for Reynolds between 700 and 2000, the best thermohydraulic behaviour would be associated with the wire-coils W01 and W02, which significantly disturb the flow with moderate increases in the friction factor in

Table II
1. Measurement accuracy, technical data provided by the manufacturer for friction factor.

Measurement	Error
Pressure Sensor	± 0,075% of the measuring range
Coriolis mass Flow meter	± 0,2% of the measurement
Tube length	± 1 mm
Tube diameter	± 0,1 mm

Table II
2. Measurement accuracy, technical data provided by the manufacturer for Nusselt number.

Measurement	Error
Voltage	±0.04% of the reading ± 0.03% of the measuring range
Intensity	±0,3% of the value
PT100 1/10 DIN Class B	0,03° C
Thermocouples (T type)	0,5° C

Table I
1. Proposed correlations for wire-coil inserts according to TSP values (Perez-Garcia et al, 2018).

Laminar fluid flow regime ($Re < Re_{CL}$)	R^2	*Av.Dev*	*Max.Dev*
$TSP < 10 (LowTSP) f_{L(L)} = 2439.936 Re^{-0.969} (p/d)^{-1.033} (e/d)^{2.928} + 14.554 Re^{-0.894}$ (I.1)	1.00	3.9%	6.4%
$10 < TSP < 750 (IntermediateTSP) e/d \leq 0.1 f_{L(Ia)} = 163.84 Re^{-0.828} (p/d)^{-0.516} (e/d)^{1.077}$ (I.2) $e/d = 0.2 f_{L(Ib)} = 13.66 Re^{-0.635} (p/d)^{-1.49}$ (I.3)	0.990.99	7.7%1.5%	12.1%1.8%
$TSP > 750 (HighTSP) f_{L(H)} = 40.568 Re^{-0.924} (p/d)^{-0.071} (e/d)^{0.426}$ (I.4)	0.99	6.5%	9.3%
Transition fluid flow regime ($Re_{CL} < Re < Re_{CT}$)	R^2	*Av.Dev*	*Max.Dev*
$TSP < 10 (LowTSP) f_{Tr(L)} = -4.68 \hat{A} \cdot 10^5 Re^{-1.261} (p/d)^{-0.0004} (e/d)^{1.91} + 2.51 \hat{A} \cdot 10^5 Re^{-1.124} (p/d)^{0.078} (e/d)^{1.998} + 0.052$ (I.5)	0.97	16.5%	23.4%
$10 < TSP < 750 (IntermediateTSP) e/d \leq 0.1 f_{Tr(Ia)} = 0.163 Re^{-0.32} (p/d)^{5.547} (e/d)^{1.057} + 1.294 Re^{0.299} (p/d)^{3.838} (e/d)^{1.606}$ (I.6) $e/d = 0.2 f_{Tr(Ib)} = Constant$	0.97	6.7%	14.1%
$TSP > 750 (HighTSP) f_{Tr(H)} = 1.12 Re^{-0.048} (p/d)^{-0.449} (e/d)^{1.061}$ (I.7)	0.96	9.2%	22.9%
Low turbulent fluid flow regime ($Re > Re_{CT}$)	R^2	*Av.Dev*	*Max.Dev*
$TSP < 10 (LowTSP) f_{T(L)} = 1442.197 Re^{-0.173} (p/d)^{1.348} (e/d)^{3.393} + 0.091 Re^{-0.037}$ (I.8)	0.99	3.1%	6.9%
$10 < TSP < 750 (IntermediateTSP) e/d \leq 0.1 f_{T(Ia)} = 7.926 Re^{-0.182} (p/d)^{-0.848} (e/d)^{1.267}$ (I.9) $e/d = 0.2 f_{T(Ib)} = 113.469 Re^{-0.409} (p/d)^{-1.819} (e/d)^{1.645}$ (I.10) $e/d = 0.286 Re > Re_{CL} f_{T(Ic)} = Eq.(11)$	0.990.99	7.7%3.3%	14.9%4.0%
$TSP > 750 (HighTSP) f_{T(H)} = 12.907 Re^{\left[-0.377 (p/d)^{-0.483}\right]} (p/d)^{-1.794} (e/d)^{0.965} + 0.297 (p/d)^{-9.528}$ (I.11)	0.96	8.4%	23.6%

relation to W03 and W04 specimens.

With this preliminary analysis, based on the analysis of the results of the friction coefficient for the four wire-coil inserts studied, it could be possible to predict the geometric characteristics of the most suitable wire-coil inserts for any application (in our work, it is applied to a harp type flat-plate solar collector). However, the definitive selection of the optimal wire-coils will be confirmed with the detailed analysis of the experimental results of heat transfer. Due to the importance of these results, they are presented in the following section.

4. Validation of the methodology through experimental heat transfer results

This section presents the results obtained from the heat transfer tests. The experimental planning was carried out in view of the friction factor curves, in order to study laminar, transition to turbulence, and low turbulence regimes for all the devices studied. The objective was to determine how the change in regime induced by the wire-coils affects the thermal behaviour of the collector, through measurements of the absorber plate temperatures and the estimation of the tube-side Nusselt number.

4.1. Absorber plate temperature

Fig. 7 summarizes the experimental results of temperature at the absorber plate at an axial location at 1290 mm, where the thermocouples were fixed as shown in Fig. 3(b). The increase of the tube-side heat transfer convective coefficient results in a decrease of the absorber temperature, fact that has a positive impact on the efficiency of a solar collector. The results for the five representative Reynolds numbers given in Table 5 are shown for the smooth tube and the four wire-coils employed.

Re = 300

In Fig. 7(a), it is shown how the only wire-coil insert that exhibits enhancement potential with respect to the smooth tube is the device W03, the wire coil with the lowest value of Re_{CL}. The specimens W01 and W02 worsen the results of the smooth tube. In solar collectors working at low Reynolds number, heat transfer in smooth tubes is enhanced by mixed convection, which may be disturbed by the secondary flows induced by the wire coils.

Re = 700

At this Reynolds number, all the wire-coils are operating above their Re_{CL}, causing a sufficiently disturbed flow to increase heat transfer in comparison with the purely laminar regime within the smooth tube. It can be observed in Fig. 7 (b) that the wire coil W03 remains exhibiting the best thermal performance ($\Delta T = 6.1\ ^{\circ}C$). The insert W04, due to its geometry, has a highly differentiated hydraulic behavior between the laminar and turbulent regime with its abrupt transition. In a turbulent regime it behaves like an artificial roughness with a separation mechanism that greatly disturbs the flow and largely increases heat transfer. But if it worked in this range of Reynold numbers in a solar collector, it would present an unstable and unpredictable behavior.

The wire-coils W01 and W02 would be working at the beginning of their transition region, the flow disturbance is moderate and as a result the increase in heat transfer is limited. The W04 begins to stand out from the rest ($\Delta T = 5.1\ ^{\circ}C$) and approaches the behaviour of W03. The inserts W01 and W02 behaves similar, with the same order of temperature decrease with respect to the smooth tube than for the two previous Reynolds numbers ($\Delta T = 3.1$ and $2.4\ ^{\circ}C$, respectively).

Re = 940

At this higher Reynolds number that exceeds significantly, for all the wire-coils studied the Re_{CL}, there is a sufficiently disturbed flow to increase the heat transfer in relation to the purely laminar regime within the smooth tube. All the inserts significantly decrease the temperature of the absorber plate. In order (from the most to the least): W03, W04, W01, W02 ($\Delta T = 6.1$, 5.4, 4.7 and $3.8\ ^{\circ}C$, respectively), Fig. 7(d).

Re = 2000

This Reynolds number was selected for the smooth tube as the upper value for laminar flow. In addition, this value is close to the estimated Re_{CT} in all the wire-coil inserts. This is therefore the value that would provide a maximum increase in heat transfer. All the inserts have a very similar absorber panel temperature. The temperature reductions are between $6\ ^{\circ}C$ and $6.7\ ^{\circ}C$. As depicted in Fig. 8, the notable increase in the convective heat transfer coefficients promoted by wire coil inserts, with values of Nusselt number significantly higher than those of the smooth tube, have a great impact on the resulting temperature in the absorber panel.

Re = 3000

The reductions in the absorber temperature regarding the smooth collector are much more moderate as shown in Fig. 7(e). This is due to the fact that in the smooth tube at this Reynolds number, the transition to turbulent regime has already taken place, and a large increase in the convection coefficients is experienced. Therefore, the enhancement potential of the wire-coil inserts is lower in this case (the temperature reductions are between $1.7\ ^{\circ}C$ and $2\ ^{\circ}C$, depending on the geometry of the insert). It should be noted that the W02 insert is now the best device from the thermal point of view along with the W03, but with a much lower level of pressure loss increase.

4.2. Peripheral temperature at section J: Nusselt number computation

Table 5 shows the Nusselt number values computed at section J together with their associated uncertainty value. The high experimental uncertainty computed is due to the small temperature difference between wall and fluid ($\overline{T_p}$-T_f). The Nusselt uncertainty can be employed to identify the onset of transition. For the specimen W03, only the Nusselt number for Re = 300 is shown, while for the smooth tube the results for all the Reynolds numbers studied are shown.

The analogy between friction factor and heat transfer is clearly depicted in Fig. 8. It shows the Nusselt number values versus the Reynolds number, for all the wire-coils studied and the smooth tube. The onset of transition for each device is clearly observed. It is observed how the wire-coil insert W03 has an outstanding behaviour, with Nu values at Re = 300 above even those reported for the smooth tube that is in mixed convection. The other wire coils show a worse thermal behaviour with respect to the smooth tube for Re = 300. For higher Reynolds numbers, Nu values for insert W03 cannot be displayed because of the experimental uncertainty. The Nusselt number remains almost constant (Nu ~ 7) up to Re = 2000 for the smooth tube. The insert W04 produces a sudden increase in the Nusselt number as observed within friction factor curve, while the devices W01 and W02 have a similar behaviour and the increments in the Nusselt number happen more gradually as the Reynolds number increase, as expected from the analysis of the extended transition region with friction coefficient almost constant.

In summary, the specimen W03 has reduced the temperature of the absorber in the range of Reynolds numbers studied. For Re from 700 to 2000 all the inserts show a better thermal behaviour regarding the smooth tube, approaching gradually as they experiment transition to the outstanding behaviour of the W03 insert. However, at Re = 2000, the values of increase of friction factor with respect to the smooth tube are very different (fw/fs ~ 8 for W01 y W02 in contrast to fw/fs = 34 for W03). For Re = 3000, the smooth tube has already undergone the transition to turbulent regime, and therefore the enhancement potential of wire-coil inserts is more limited.

The final selection depends on the operating Reynolds number range of the equipment. The wire-coils employed must have a Re_{CL} lower than this range. The maximum enhancement is obtained for equipment working in a laminar regime at a Reynolds number close to the Re_{CT} of the selected wire-coil. If the equipment is expected to work in a wide Reynolds number range, it is convenient to choose inserts whose Re_{CL}-Re_{CT} interval lies here and that provide a stable behaviour within this

region. The wire-coils like the W04 should be discarded, when its critical transition Reynolds number falls into the operating range of the equipment, as they would present an unpredictable/unstable behaviour. If the pressure loss is important, a wire-coil with a stable behaviour and with the lower friction loss associated should be chosen. If the thermal equipment does not present restrictions in terms of pressure loss and the final aim is exclusively to maximize heat transfer, the specimen with stable behaviour and a higher level of friction (greater associated disturbance in the flow) could be chosen. For the equipment studied (a harp type solar collector) located in Cartagena (Southeast of Spain 37°36′ N, 0°59′ W) working with a moderate glycol mixture at a wide Reynolds numbers range from 300 to 2000, a feasible option would be the wire-coil W03, since it promotes a perturbed regime throughout the working range and the friction in this case is not decisive since the collector only represents a small fraction of the total pressure loss in the forced circulation installation.

5. Conclusions

- The methodology proposed is based on the fact that the optimal wire-coil for a given application will be the one that due to its geometric characteristics develops an extended transition region that is as wide as possible, and that adjusts to the range of Reynolds numbers of the application under study, also maintaining a coefficient of friction as low as possible and constant. For the pre-selection of the adequate wire-coil geometry to insert, the non-dimensional parameter *TSP* is computed.
- The methodology has been validated for a representative thermal application, a harp-type flat-plate solar collector. The thermo-hydraulic behaviour of four wire-coil inserts with different geometries has been studied. The inserts analyzed exhibited significant differentiated behaviours in their friction factor curves and critical Reynolds numbers Re_{CL} and Re_{CT}, according to the Transition Shape Parameter values selected; $TSP_{W01} = 759$, $TSP_{W02} = 196$, $TSP_{W03} = 35.3$ and $TSP_{W04} = 3,1$
- All the inserts advance the transition at much lower values of Reynolds number than the smooth tube, from $Re_{CL(W03)} = 364$ to $Re_{CL(W02)} = 663$ depending on their geometry, and present an extended transition region with a nearly constant friction factor (except for the W04) up to $Re_{CT(W01)} = 2516$, $Re_{CT(W02)} = 2286$ and $Re_{CT(W03)} = 2324$. The obtained experimental friction factor results have shown values of critical Reynolds numbers, in agreement with those predicted by the proposed correlations from Pérez-García et al [21] (relative errors of 2.5 % for Re_{CL} and 8.6 % for Re_{CT}).
- The increase in the friction coefficient produced by the wire-coils, based on their geometry, has a limited influence on the pumping power required, since depending on the type of application it can represent a very low percentage in relation to the total losses of the whole installation, this is the case for a harp-type flat-plate solar collector. For the four wire-coils studied, and within the range of Reynolds numbers between 300 and 3000, the results obtained are: $\bar{f}_{W01}/\bar{f}_s = 4.3$, $\bar{f}_{W02}/\bar{f}_s = 3.82$, $\bar{f}_{W03}/\bar{f}_s = 18.84$ and $\bar{f}_{W04}/\bar{f}_s = 7.94$
- Given the direct relationship between hydraulic and thermal behaviour, the information provided by the TSP is of great value, since it allows to define very precisely the different flow regions. Once these are established, the thermal behaviour of a specific geometry in each region can be qualitatively inferred allowing the selection of the optimal insert when several geometries are available.
- The experimental results of heat transfer obtained for the validation of the proposed methodology indicate that within the range of Reynolds numbers between 300 and 3000, the wire-coil WO3 due to its low $Re_{CL(W03)} = 364$ produces an enhancement in heat transfer in all cases and, therefore, a reduction in the absorber temperature. The maximum difference is encountered at $Re = 2000$ and of approximately $\Delta t = 6$ °C, which represents a 15.8 % with respect to the temperature of the absorber with a smooth tube. The rest of the wire-coils studied, as they present a higher Re_{CL} improve heat transfer from Re = 700, promoting a different reduction in the absorber temperature depending on its geometric characteristics. It is noteworthy that at Re = 2000 the differences measured in the absorber temperature are similar for the four wire-coils studied.
- Regarding the Nusselt number, measured at section J, located at a distance of 1.61 m from the riser entrance ($x_J = 0,85L_{riser}$), it is worthy to mention that, while in the smooth tube the Nusselt number remains constant at an approximate value of 7 up to Re = 2000, the four wire-coils produce a significant enhancement, being the average ratios $\overline{Nu}_{W01}/\overline{Nu}_s = 2.67$, $\overline{Nu}_{W02}/\overline{Nu}_s = 2.38$ (excluding the ratios $\overline{Nu}_{W03}/\overline{Nu}_s$ and $\overline{Nu}_{W04}/\overline{Nu}_s$ that due to the high uncertainty could not be evaluated in the entire range of Reynolds numbers).
- The results show how the wire-coil inserts with a constant friction factor in the transition region have a better thermal behaviour when they operate in this region. Thus, in order to choose the optimal wire coil insert for a given application where there is information about the operating Reynolds numbers and the characteristic diameter of the tubes, a wire-coil with ratios p/d and e/d with $e/d \leq 0.1$ should be selected to obtain an intermediate TSP range ($10 < TSP < 750$). The best option (appropriate value) will depend on the importance of the increase in pressure losses. In applications where pressure loss is not a limiting factor, an e/d ratio in the range $0.1 < e/d \leq 0.2$could also be chosen. Once the TSP has been obtained, and through the appropriate correlations, the critical Reynolds numbers Re_{CL} and Re_{CT} could be obtained (to verify that the obtained interval fits within the operating range of the application under study), and also the average friction factor in the extended transition region $[Re_{CL} - Re_{CT}]$.

Declaration of Competing Interest

The authors declare that they have no known competing financial interests or personal relationships that could have appeared to influence the work reported in this paper.

Data availability

Data will be made available on request.

Acknowledgement

The authors gratefully acknowledge to European Regional Development Fund and Ministerio de Ciencia e Innovación - Agencia Estatal de Investigación for the financial support of the project ALTES: “Active Latent Thermal Energy Storage”, Ref. PGC2018-100864-B-C21.

Annex I. Proposed friction factor correlations for wire-coil inserts according to TSP values

See Table I.1

Annex II. Uncertainty analysis

II.1. Calculation of the uncertainty of the friction factor

The Fanning friction factor is given by Eq (II.1) as a function of directly measured magnitudes,

$$f = \frac{d}{2l_p}\frac{\Delta p}{\rho U^2} = \frac{\rho\pi^2}{32}\frac{d^5}{l_p}\frac{\Delta p}{G^2} \tag{II.1}$$

The total uncertainty of the calculation of the friction factor $u_{f(T)}$ is due to the accuracy of the measuring instruments u_f and to the standard deviation of the measurements made σ_f (Eq. II.2)

$$u_{f(T)} = \sqrt{(u_f)^2 + (\sigma_f)^2} \tag{II.2}$$

Being,

$$u_f^2 = \left(\frac{\partial f}{\partial \Delta p}\right)^2 u_{\Delta_p}^2 + \left(\frac{\partial f}{\partial G}\right)^2 u_G^2 + \left(\frac{\partial f}{\partial D}\right)^2 u_d^2 + \left(\frac{\partial f}{\partial l_p}\right)^2 u_{l_p}^2 \tag{II.3}$$

Table II.1 shows the main uncertainties that have been taken into account when calculating the uncertainty of the friction factor.

II.2. Calculation of the uncertainty of the Nusselt number

The Nusselt number is given by Eq. (II.4) depending on the magnitudes measured directly,

$$Nu = \frac{hD}{k} = \frac{q''}{T_w - T_f}\frac{d}{k} = \frac{1}{\pi l_p k}\frac{V\,I}{(T_w - T_f)} \tag{II.4}$$

The total uncertainty of the calculation of the Nusselt number $u_{Nu(T)}$ is due to the accuracy of the measuring instruments u_{Nu} and to the standard deviation of the measurements made σ_{Nu} (Eq. II.2)

$$u_{Nu(T)} = \sqrt{(u_{Nu})^2 + (\sigma_{Nu})^2} \tag{II.5}$$

Being,

$$u_{Nu}^2 = \left(\frac{\partial Nu}{\partial V}\right)^2 u_V^2 + \left(\frac{\partial Nu}{\partial I}\right)^2 u_I^2 + \left(\frac{\partial Nu}{\partial T_w}\right)^2 u_{T_w}^2 \left(\frac{\partial Nu}{\partial T_f}\right)^2 u_{T_f}^2 + \left(\frac{\partial Nu}{\partial l_p}\right)^2 u_{l_p}^2 \tag{II.6}$$

The Table II.2 shows the technical data provided by the manufacturer since the measurement accuracies of the primary magnitudes are involved:

References

[1] M.A. Akhavan-Behabadi, R. Kumar, M.R. Salimpour, R. Azimi, Pressure drop and heat transfer augmentation due to coiled wire inserts during laminar flow of oil inside a horizontal tube, Int. J. Therm. Sci. 49 (2010) 373–381, https://doi.org/10.1016/j.icheatmasstransfer.2015.02.013.

[2] K. Balaji, K.P. Ganesh, D. Sakthivadivel, V.S. Vigneswaran, S. Iniyan, Experimental investigation on flat plate solar collector using frictionally engaged thermal performance enhancer in the absorber tube, Renewable Energy 142 (2019) 62–72, https://doi.org/10.1016/j.renene.2019.04.078.

[3] L. Chen, H.J. Zhang, Convection Heat Transfer Enhancement of Oil in a Circular Tube With Spiral Spring Inserts, Heat Transfer Meas. Anal. ASME 249 (1993) 45–50.

[4] L.A.J. Deeyoko, K. Balaji, S. Iniyan, C. Sharmeela, Exergy, economics and pumping power analyses of flat plate solar water heater using thermal performance enhancer in absorber tube, Appl. Therm. Eng. 154 (2019) 726–737, https://doi.org/10.1016/j.applthermaleng.2019.03.135.

[5] J.A. Duffie, W.A. Beckman, N. Blair, Solar Engineering of Thermal Processes, Photovoltaics and Wind: Photovoltaics and Wind, 5th ed., John Wiley and Sons, New Jersey, 2020.

[6] A. García, P.G. Vicente, A. Viedma, Experimental Study of Heat Transfer Enhancement with Wire-coil Inserts in Laminar, Transition, and Turbulent Regimes at Different Prandtl Numbers, Int. J. Heat and Mass Transfer, 48 (2005): 4640–4651. https://doi.org/10.1016/j.ijheatmasstransfer.2005.04.024.

[7] A. García, J.P. Solano, P.G. Vicente, A. Viedma, Flow Patterns Assessment in Tubes with Wire-coil Inserts in Laminar and Transition Regimes, Int. J. Heat and Fluid Flow, 28 (2007): 516-525 https://doi.org/10.1016/j.ijheatfluidflow.2006.07.001.

[8] A. Garcia, J.P. Solano, P.G. Vicente, A. Viedma, Enhancement of laminar and transitional flow heat transfer in tubes by means of wire coil inserts, Int. J. Heat Mass Transf. 50 (15–16) (2007) 3176–3189, https://doi.org/10.1016/j.ijheatmasstransfer.2007.01.015.

[9] A. García, J.P. Solano, P.G. Vicente, A. Viedma, The influence of artificial roughness shape on heat transfer enhancement: Corrugated tubes, dimpled tubes and wire coils, Appl. Therm. Eng. 35 (2012) 196–201, https://doi.org/10.1016/j.applthermaleng.2011.10.030.

[10] S. Gunes, V. Ozceyhan, O. Buyukalaca, Heat transfer enhancement in a tube with equilateral triangle cross sectioned coiled wire inserts, Exp. Therm Fluid Sci. 34 (6) (2010) 684–691, https://doi.org/10.1016/j.expthermflusci.2009.12.010.

[11] K.A. Hamid, W.H. Azmi, R. Mamat, K.V. Sharma, Heat transfer performance of TiO2–SiO2 nanofluids in a tube with wire coil inserts, Appl. Therm. Eng. 152 (2019) 275–286, https://doi.org/10.1016/j.applthermaleng.2019.02.083.

[12] Y. Hong, J. Du, S. Wang, S. Huang, W. Ye, Heat transfer and fluid flow behaviors in a tube with modified wire coils, Int. J. Heat Mass Transf. 124 (2018) 1347–1360, https://doi.org/10.1016/j.ijheatmasstransfer.2018.04.017.

[13] H. Inaba, K. Ozaki, S. Kanakoa, A Fundamental Study of Heat Transfer Enhancement and Flow-Drag Reduction in Tubes by Means of Wire-coil Insert, Japan Soc. Mech. Eng. 60 (1994) 240–247, https://doi.org/10.1299/kikaib.60.1005.

[14] M.R. Jafari Nasr, A. Habibi Khalaj, S.H. Mozaffari, Modelling of Heat Transfer Enhancement by Wire-coil Inserts Using Artificial Neural Network Analysis, Appl. Therm. Eng. 30 (2010): 143-151. https://doi.org/10.1016/j.applthermaleng.2009.07.014.

[15] A. Jamar, Z.A.A. Majid, W.H. Azmi, M. Norhafana, A.A. Razak, A review of water heating system for solar energy applications, Int. Commun. Heat Mass Transfer 76 (2016) 178–187, https://doi.org/10.1016/j.icheatmasstransfer.2016.05.028.

[16] M.R. Kalateh, A. Kianifar, M. Sardarabadi, A three-dimensional numerical study of the effects of various twisted tapes on heat transfer characteristics and flow field in a tube: Experimental validation and multi-objective optimization via response surface methodology, Sustainable Energy Technol. Assess. 50 (2022), 101798, https://doi.org/10.1016/j.seta.2021.101798.

[17] B. Kumar, G.P. Srivastava, M. Kumar, A.K. Patil, A review of heat transfer and fluid flow mechanism in heat exchanger tube with inserts, Chem. Eng. Process. - Process Intensification 123 (2018) 126–137, https://doi.org/10.1016/j.cep.2017.11.007.

[18] P. Naphon, Effect of coil-wire insert on heat transfer enhancement and pressure drop of the horizontal concentric tubes, Int. Commun. Heat Mass Transfer 33 (6) (2006) 753–763, https://doi.org/10.1016/j.icheatmasstransfer.2006.01.020.

[19] Y.G. Nazmeev, A.M. Konakhin, B.A. Kumirov, O.P. Shinkevich, An Experimental Study of Heat Transfer under Laminar Flow Conditions in Tubes with Spiral-Wire Inserts, Therm. Eng. 41 (11) (1994) 898–901.

[20] K.M. Pandey, R. Chaurasiya, A review on analysis and development of solar flat plate collector, Renew. Sustain. Energy Rev. 67 (2017) 641–650.

[21] J. Pérez-García, A. García, R. Herrero-Martín, J.P. Solano, Experimental correlations on critical Reynolds numbers and friction factor in tubes with wire-coil

inserts in laminar, transitional and low turbulent flow regimes, Exp. Therm Fluid Sci. 91 (2018) 64–79, https://doi.org/10.1016/j.expthermflusci.2017.10.003.
[22] P. Promvonge, Thermal performance in circular tube fitted with coiled square wires, Energy Convers. Manage. 49 (5) (2008) 980–987, https://doi.org/10.1016/j.enconman.2007.10.005.
[23] P. Promvonge, P. Promthaisong, S. Skullong, Experimental and numerical thermal performance in solar receiver heat exchanger with trapezoidal louvered winglet and wavy groove, Sol. Energy 236 (2022) 153–174, https://doi.org/10.1016/j.solener.2022.02.052.
[24] S. Roy, S.K. Saha, Thermal and Friction Characteristics of Laminar Flow Through a Circular Duct Having Helical Screw-tape with Oblique Teeth Inserts and Wire-coil Inserts, Exp. Therm Fluid Sci. 68 (2015) 733–743, https://doi.org/10.1016/j.expthermflusci.2015.07.007.
[25] S. Sadhishkumar, T. Balusamy, Performance improvement in solar water heating systems—A review, Renew. Sustain. Energy Rev. 37 (2014) 191–198, https://doi.org/10.1016/j.rser.2014.04.072.
[26] S.K. Saha, H. Ranjan, M.S. Emani, A.K. Bharti, Displaced Enhancement Devices and Wire Coil Inserts, in: Insert Devices and integral Roughness in Heat Transfer Enhancement. SpringerBriefs in Applied Sciences and Technology, Springer, Cham, 2020, https://doi.org/10.1007/978-3-030-20776-2_3.
[27] S.A. Sakhaei, M.S. Valipou, Performance enhancement analysis of the flat plate collectors: A comprehensive review, Renew. Sustain. Energy Rev. 102 (2019) 186–204, https://doi.org/10.1016/j.rser.2018.11.014.
[28] J. San, W. Huang, C. Chen, Experimental investigation on heat transfer and fluid friction correlations for circular tubes with coiled-wire inserts, Int. Commun. Heat Mass Transfer 65 (2015) 8–14, https://doi.org/10.1016/j.icheatmasstransfer.2015.04.008.
[29] R. Sethumadhavan, M. Raja Rao, Turbulent Flow Heat Transfer and Fluid Friction in Helical-Wire-Coil-Inserted Tubes, Int. J. Heat and Mass Transfer 26 (1983) 1833–1845, https://doi.org/10.1016/S0017-9310(83)80154-9.
[30] M.A. Sharafeldeen, N.S. Berbish, M.A. Moawed, R.K. Ali, Experimental investigation of heat transfer and pressure drop of turbulent flow inside tube with inserted helical coils, Heat Mass Transf. 53 (4) (2017) 1265–1276.
[31] K. Sharifi, M. Sabeti, M. Rafiei, A.H. Mohammadi, A. Ghaffari, M.H. Asl, H. Yousefi, A good contribution of computational fluid dynamics (CFD) and GA-ANN methods to find the best type of helical wire inserted tube in heat exchangers, Int. J. Therm. Sci. 154 (2020), 106398, https://doi.org/10.1016/j.ijthermalsci.2020.106398.
[32] A.N. Skrypnik, A.V. Shchelchkov, Y.F. Gortyshov, I.A. Popov, Artificial neural networks application on friction factor and heat transfer coefficients prediction in tubes with inner helical-finning, Appl. Therm. Eng. 206 (2022), 118049, https://doi.org/10.1016/j.applthermaleng.2022.118049.
[33] A. Subasi, K. Erdem, An integrated optimization methodology for heat transfer enhancement: A case study on nanofluid flow in a pipe equipped with inserts, Int. J. Heat Mass Transf. 172 (2021), 121187, https://doi.org/10.1016/j.ijheatmasstransfer.2021.121187.
[34] G. Verma, S. Singh, S. Chander, P. Dhiman, Numerical investigation on transient thermal performance predictions of phase change material embedded solar air heater, J. Storage Mater. 47 (2022), 103619, https://doi.org/10.1016/j.est.2021.103619.
[35] E. Vengadesan, R. Senthil, A review on recent development of thermal performance enhancement methods of flat plate solar water heater, Sol. Energy 206 (2020) 935–961, https://doi.org/10.1016/j.solener.2020.06.059.
[36] C.S. Wang, C.C. Chen, W.C. Chang, T.M. Liou, Experimental studies of turbulent pulsating flow and heat transfer in a serpentine channel with winglike turbulators, Int. Commun. Heat Mass Transfer 131 (2022), 105837, https://doi.org/10.1016/j.icheatmasstransfer.2021.105837.
[37] L. Wang, B. Sunden, Performance comparison of some tube inserts, Int. Commun. Heat Mass Transfer 29 (1) (2002) 45–56, https://doi.org/10.1016/S0735-1933(01)00323-2.
[38] R.L. Webb, N.-H. Kim, Principles of Enhanced Heat Transfer, CRC Press, 2nd Edition, 2005.
[39] Y.F. Zhang, F.Y. Li, Z.M. Liang, Heat Transfer in Spiral-Coiled-. Inserted Tubes and its Applications, in Advances in Heat Transfer. Augmentation and Mixed Convection, ASME HTD-Vol.169, pp. 31-. 36, 1991.